BRAIN COMMUNICATIONS

Higher white matter hyperintensity lesion load is associated with reduced long-range functional connectivity

Fanny Quandt, Felix Fischer, Julian Schröder, Marlene Heinze, Iris Lettow, Benedikt M. Frey, Simon S. Kessner, Maximilian Schulz, Focko L. Higgen, Bastian Cheng, Christian Gerloff and Götz Thomalla

Cerebral small vessel disease is a common disease in the older population and is recognized as a major risk factor for cognitive decline and stroke. Small vessel disease is considered a global brain disease impacting the integrity of neuronal networks resulting in disturbances of structural and functional connectivity. A core feature of cerebral small vessel disease commonly present on neuroimaging is white matter hyperintensities. We studied high-resolution resting-state EEG, leveraging source reconstruction methods, in 35 participants with varying degree of white matter hyperintensities without clinically evident cognitive impairment in an observational study. In patients with increasing white matter lesion load, global theta power was increased independently of age. Whole-brain functional connectivity revealed a disrupted network confined to the alpha band in participants with higher white matter hyperintensities lesion load. The decrease of functional connectivity was evident in long-range connections, mostly originating or terminating in the frontal lobe. Cognitive testing revealed no global cognitive impairment; however, some participants revealed deficits of executive functions that were related to larger white matter hyperintensities lesion load. In summary, participants without clinical signs of mild cognitive impairment or dementia showed oscillatory changes that were significantly related to white matter lesion load. Hence, oscillatory neuronal network changes due to white matter lesions might act as biomarker prior to clinically relevant behavioural impairment.

Department of Neurology, University Medical Center Hamburg-Eppendorf, Germany

Correspondence to: Dr. Fanny Quandt
Department of Neurology Martinistr. 52, 20246 Hamburg, Germany
E-mail: f.quandt@uke.de

Keywords: microangiopathy; leukoaraiosis; cerebral small vessel disease; EEG; imaginary coherence

Abbreviations: MMSE = Mini-Mental State Examination; ROI = region of interest; SVD = small vessel disease; TMT-B = trail-making test B; WMH = white matter hyperintensities

Received February 18, 2020. Revised June 8, 2020. Accepted June 12, 2020. Advance Access publication July 20, 2020

Graphical Abstract

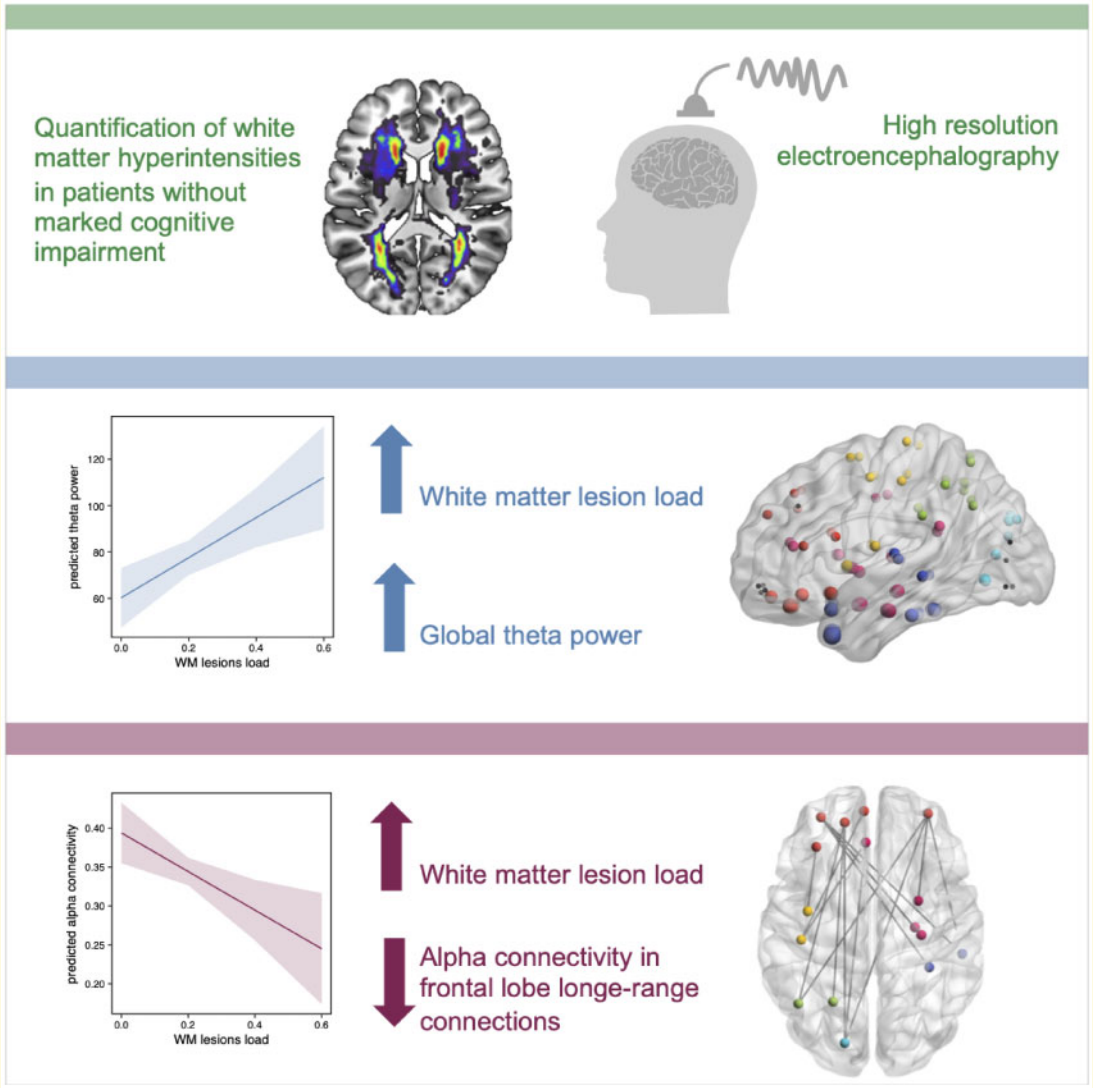

Introduction

Cerebral small vessel disease (SVD) is the most common vascular cause of dementia and increases the risk of stroke (Pantoni, 2010). White matter hyperintensities (WMH) are the most prominent feature of SVD on magnetic resonance imaging (MRI) (Wardlaw *et al.*, 2013). The prevalence of WMH in the older population is almost ubiquitous (de Leeuw, 2001), and age is a consistent risk factor for WMH (Habes *et al.*, 2016). Moreover, WMH are associated with increased risk of cognitive decline (Carmichael *et al.*, 2010).

In vascular dementia, in contrast to Alzheimer's Disease, memory is initially preserved and deficits comprise executive function and processing speed (Román *et al.*, 2002). The disconnection of distant brain regions leads to an impairment of network functioning and results in cognitive dysfunction characteristic to vascular dementia. WMH most commonly lie in periventricular regions affecting the white matter tracts, evoking network changes of white matter structural connections in patients with SVD (Lawrence *et al.*, 2014; Kim *et al.*, 2015; Tuladhar *et al.*, 2016). Furthermore, SVD has been shown to impact functional networks and reduce functional connectivity in functional-MRI (fMRI) studies (Schaefer *et al.*, 2014). Only a few studies in patients with SVD investigated oscillatory functional connectivity using EEG and by this bypassing the haemodynamical dependency of the blood oxygenation level dependent (BOLD) signal which is known to be affected by cerebrovascular disease and thus might confound connectivity measurements based on fMRI (van Straaten *et al.*, 2015). While there exists a vast literature of oscillatory changes in patients with neurodegenerative disease, especially Alzheimer's Disease (Jeong, 2004), electrophysiological

studies in patients with WMH without global cognitive impairment or Alzheimer's Disease are scarce.

A previous study, analysing 14 EEG channels in healthy older participants, reported intermittent temporal slowing of neural oscillatory activity that was present in 50% of the older participants. This slowing was related to the presence of WMH on MRI (Oken and Kaye, 1992). A more recent study in patients with WMH confirmed an increase of power in slow oscillatory activity opposed by a decrease of power in alpha/beta frequency range, a pattern often seen in patients with Alzheimer's Disease as well (van Straaten *et al.*, 2012). Patients in this study, however, already showed global cognitive impairment and were diagnosed with vascular dementia. Likewise, most previous studies assessing network pathology in SVD have mainly investigated patients that already displayed clinical symptoms of cognitive decline. It is not known whether changes in oscillatory connectivity of brain networks are also present in pre-clinical stages of SVD, similar to reversible functional connectivity changes described recently for asymptomatic stenotic large artery disease (Quandt *et al.*, 2019).

Hence, in this study, we aimed at assessing oscillatory network changes depending on WMH in patients without clinical signs of mild cognitive impairment or dementia. We recorded high-density EEG at rest and made use of source reconstruction methods to assess whole-brain functional connectivity. This approach offers the benefit to obtain functional connectomes based on the automated anatomical labelling atlas, that are comparable to previously published structural connectomes in patients with WMH. Moreover, source reconstruction reduces the influence of volume conduction which is present in former sensor-level EEG studies. White matter lesion load was obtained from individual MRI scans and cognitive function was evaluated in order to assess whether patients already showed cognitive deficits. Similar to the known structural network disturbances in patients with SVD, we hypothesize that WMH are associated with alterations of oscillatory functional connectivity, even in the absence of cognitive impairment.

Materials and methods

Participants and neuropsychological testing

Thirty-nine participants were enrolled at the Department of Neurology, University Medical Center Hamburg-Eppendorf, Germany. These included 19 participants with obvious WMH that had become apparent on prior clinical imaging (CT or MRI) and 20 participants with no history of SVD. The participants without a history of SVD were previously included as a control group for a study in patients with asymptomatic internal carotid artery stenosis (Quandt *et al.*, 2019). All participants underwent EEG recording, structural MR imaging, neurologic and neuropsychologic examination, and clinical history taking. All data recordings were performed between October 2015 and November 2016. From the participants with obvious WMH, three participants had to be excluded due to extensive artefacts during EEG recordings and one participant was excluded due to extensive artefacts in MR imaging. Thus, finally, 35 subjects were included in the analysis. All participants were above 50 years of age, German native speakers, and did not have a history or obvious clinical signs of cognitive impairment, did not self-report any cognitive deficits, no history of any severe neuropsychiatric disease, dementia, depression or significant neurological symptoms. Moreover, the participants did not take any psychotropic medication.

Neuropsychological testing was obtained in all participants in the German language, including the Mini-Mental State Examination (MMSE) and tests of executive function [trail-making test (TMT) B and Stroop colour-word test]. Z-scores of TMT-B results, corrected for age, education and sex were calculated according to CERAD-Plus Online (https://www.memory-clinic.ch/de/main-navigation/neuropsychologen/cerad-plus/auswertungprogramme/cerad-plus-online/, accessed 29 July 2020). By subtracting the time to accomplish the Stroop colour-word test, results were obtained that were modified according to the age of each participant by assessment tables from the Nürnberger Alters-Inventar resulting in C-scores (Oswald and Fleischmann, 1997).

All participants provided written informed consent according to the Declaration of Helsinki. The study was approved by the local ethics committee of the Medical Association of Hamburg.

Recording and preprocessing

Electroencephalography

Resting-state EEG data were recorded in participants seated in front of a screen for ~15 min. Participants were asked to visually fixate a cross presented on the screen in order to avoid drowsiness. Data were sampled at 1000 Hz using a 63-channel EEG system positioned according to the 10–10 System of the American Electroencephalographic Society (using actiCAP®, Brain Products GmbH, Germany, Gilching; Electro-Cap International, Inc., Eaton, OH, USA) and referenced to the Cz electrode. The impedance of the EEG electrodes was kept below 25 kΩ. Data were segmented into 4 s epochs for further analysis, filtered from 2 to 256 Hz with a bandpass-filter of fourth order and a bandstop filter at 49–51 Hz, 99–101 Hz and 149–151 Hz. Epochs with artefactual amplitude steps were dismissed from the analysis after automatic detection and subsequent visual inspection and noisy channels were interpolated. Eye-movement artefacts were removed employing an independent component analysis (Makeig *et al.*, 1996).

Subsequently, data were resampled to 125 Hz and re-referenced to a common average reference. Artefact rejection resulted in an overall number of μ = 199.7/206.5, standard deviation (SD) = 32.3/24.2 trials (participants with lesions/without lesions). The Fieldtrip toolbox (Oostenveld *et al.*, 2011) as well as custom-written software using MATLAB Version 8.2.0 (R2013b, Mathworks Inc. MA, USA) were used for EEG data processing.

Brain imaging

High-resolution T1-weighted anatomical images data were acquired using a 3 T Siemens Skyra MRI scanner (Siemens, Erlangen, Germany). The MRI protocol included, among others, T1 MPRage (flip angle = 9°, time of repetition (TR) = 2500 ms, echo time (TE) = 2.12 ms, slice thickness = 0.9 mm, inversion time 1100 ms, matrix = 232 × 288, field of view (FOV) = 193 mm × 293 mm) and a fluid attenuated inversion recovery (FLAIR) sequence (flip angle = 150°, TR = 9000 ms, TE = 90 ms, slice thickness = 5 mm, inversion time- = 2500 ms, matrix = 320 × 270, FOV = 194 mm × 230 mm).

Data analysis

Source reconstruction and connectivity analysis

Forward models were calculated based on individual T1-weighted structural MRIs and individual electrode positions registered with an ultrasound localization system (CMS20, Zebris, Isny, Germany). A Boundary Element Method volume conduction model (Fuchs *et al.*, 2002) was used for the forward solution using the Statistical Parametric Mapping software (SPM12b, Wellcome Trust Centre for Neuroimaging, London, UK, http://www.fil.ion.ucl.ac.uk/spm, accessed 29 July 2020). We computed linearly constrained minimum variance beamformer coefficients from the time series for each of the voxels on a 6-mm grid covering the brain (Van Veen *et al.*, 1997). These linearly constrained minimum variance weights were used for the later projection of complex Fourier spectra into source space. The optimal dipole orientation for each voxel was computed using the singular value decomposition. The template brain was parcellated into 90 anatomical areas based on the automated anatomical labelling atlas (Tzourio-Mazoyer *et al.*, 2002), excluding the cerebellar parcellation.

Complex sensor-level Fourier spectra were calculated by applying a Fast Fourier Transformation using one Hanning taper. Fourier spectra were obtained for the delta (centre frequency = 3 Hz, frequency smoothing = 1 Hz), theta (centre frequency = 6 Hz, frequency smoothing = 2 Hz), alpha (centre frequency = 10 Hz, frequency smoothing = 2 Hz) and beta band (centre frequency = 19 Hz, frequency smoothing = 5 Hz). Afterwards, complex spectra for each epoch were projected into source space using the linearly constrained minimum variance beamformer coefficients. For each voxel, the real-valued power was calculated from the complex Fourier spectra. The complex-valued spectra were retained for subsequent connectivity analysis. For automated anatomical labelling atlas parcellation, single-epoch spectral data were averaged across all voxels within one automated anatomical labelling atlas region. Afterwards, the absolute imaginary part of the coherence was calculated between all 90 region of interests (ROI) resulting in a 90 × 90 connectivity matrix. We chose the imaginary part of the coherence to reduce the false connectivity arising from volume conduction (Nolte *et al.*, 2004). For power analysis, epochs were averaged in each ROI resulting in a 90 × 1 power vector. Plots were generated with BrainNet Viewer (Xia *et al.*, 2013) as well as the circlize package in R version 3.6.1(Gu *et al.*, 2014).

Analysis of white matter hyperintensity lesion load

For segmentation of WMH, T1- and T2-weighted MRI scans were semi-automatically segmented using the Clusterize-Toolbox for spm8 (Clas *et al.*, 2012). The preprocessed masks were corrected manually by an experienced investigator. To account for interindividual differences in brain volume, WMH lesion load was calculated as the ratio of WMH volume and whole-brain volume.

For illustrative purposes, segmented WMH lesion mask was projected to a standard brain template in Montreal Neurological Institute (MNI) 152 space. Individual FLAIR images were registered to a structural T1-weighed image in MNI space via linear and non-linear registration as implemented in the FMRIB Software Library toolbox [Version 6.0, http://www.fmrib.ox.ac.uk/fsl, accessed 29 July 2020 (Jenkinson *et al.*, 2012)]. Resulting warp fields were applied to lesion masks for transferring WMH lesion masks to MNI 152 standard space and added to illustrate WMH lesion frequency and distribution. Segmentation of the hippocampus was performed using Freesurfer [Version 6.0, https://surfer.nmr.mgh.harvard.edu/, accessed 29 July 2020 (Fischl *et al.*, 2002)] with standardized pipelines ('recon-all'). Hippocampus volumes were extracted from automated segmentation statistics ('aseg.stats') after visual verification of correct segmentations and manual corrections, if necessary.

Statistical analysis

We constructed multiple linear models using the R statistical package version 3.6.1. To assess the relationship between cognition and WMH lesion load, linear models were calculated for each neuropsychological test ($n = 3$) as a function of lesion load. The relationship of spectral power and WMH lesion load was modelled in each ROI ($n = 90$) for each frequency band ($n = 4$) independently. Similarly, the relationship between the connectivity (imaginary coherence) and WMH lesion load was modelled for each connection [$n = 90*(90 - 1)/2 = 4005$) and for each frequency band ($n = 4$) independently. EEG features

and WMH lesion load were transformed by the third root to obtain a closer to normal distribution. Age has been shown to highly influence cognitive function (Habes *et al.*, 2016) as well as oscillatory activity (Quandt *et al.*, 2016), thus we included age as a fixed effect in each model (except for the cognitive model of Stroop and TMT-B test as these values were already corrected for age). *P*-values of the F-statistic were adapted for multiple comparisons by false discovery rate (FDR) correction. Global network effects were analysed with linear-mixed model analyses (package lme4). These models contained the fixed effects 'WMH lesion load' and 'age'. As additional random effects, we included intercepts for ROI or connection respectively and by-patient variability. Mixed model *P*-values were obtained by analysis of variance and estimates are reported with 95% confidence intervals.

Data availability

Data and code used for the analysis are available upon reasonable request from the corresponding author.

Results

Participants' characteristics and results of neurophysiological testing

The distribution of white matter lesion load and age for all participants is shown in Fig. 1. Participants had a mean age of 68.77 years (±9.4 SD, range 51–84). Twelve of the 35 participants were female.

White matter lesions included periventricular white matter changes as well as subcortical changes (see Fig. 2 for a heat map of WMH probability). According to the STRIVE criteria (Wardlaw *et al.*, 2013), five participants showed a lacune of presumed vascular origin (four participants with one lacune, one participant with two lacunes), none of which were symptomatic.

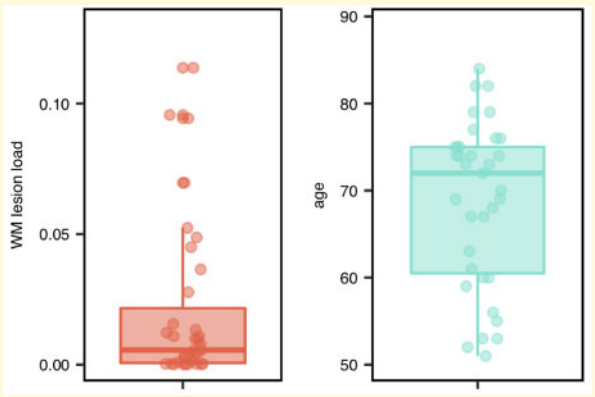

Figure 1 WMH lesion load and age of all participants. Left column depicts the WMH lesion load ratio. Right column depicts the age distribution. Boxplots depict median and 25%/75% quantile; points show individual data.

Participants did not show any global cognitive impairment (median MMSE = 29, range 25–30). Three participants, however, presented with a MMSE score of 25, which might already point to mild dementia. Executive functions revealed deficits in some patients (please refer to Fig. 3 for TMT-B z-scores and Stroop C-scores). A linear regression analyses in order to explain cognitive function by WMH lesion load revealed a worse performance in executive functions with increasing lesion load for Stroop [$F(1,33) = 5.063$, $P_{\text{lesion load}} = 0.0312$, $R^2 = 0.13$] and TMT-B [$F(1,33] = 6.48$, $P_{\text{lesion load}} = 0.009$, $R^2 = 0.16$]. Global cognitive function assessed by MMSE did not show a significant dependence on lesion load, when corrected for age [$F(2,32) = 1.682$, $P_{\text{lesion load}} = 0.70$, $R^2 = 0.095$] (Fig. 3).

Increase of oscillatory power

We aimed to explore oscillatory power depending on WMH lesion load. In an exploratory approach, we performed multiple linear regression analyses in order to explain power by WMH lesion load, corrected for age. We iteratively tested the model for each frequency band (delta, theta, alpha and beta) and region (90 ROIs). Only theta power was explained by WMH lesion load. Theta power was almost globally increased with higher lesion load (FDR corrected for ROIs = 90, $P_{\text{corrected}} < 0.05$, see Fig. 4A). Highest mean model estimates of theta power were found in ROIs belonging to the temporal lobe. Age did not add significant variance to theta power after correction for multiple comparisons. A linear-mixed model analysis with additional random effects for ROI and by-patient variability, confirmed a global increase of theta power with increasing lesion load [$F(1,34.76) = 10.48$, $P = 0.0027$, Fig. 4B]. All other models for the delta, alpha and beta band were not significant, even before correction of multiple comparisons (for all uncorrected *P*-values of overall models, please refer to Supplementary Fig. 1). When calculating the linear-mixed model further including cognitive function as a fixed effect (either MMSE, TMT-B or Stroop) the fixed effect 'cognitive function' was not significant. Hence, neither global cognitive function nor executive functions, but only WMH lesion, added to the explanation of variance to theta power. Furthermore, in order to evaluate whether the hippocampus volume influences theta power, we included the mean hippocampus volume from the left and right hippocampus of each participant as a fixed effect into the linear-mixed model. Hippocampus volume, however, in contrast to WMH lesion load, was not significant, hence did not explain theta power (please refer to Supplementary Fig. 2 for hippocampus volumes and Supplementary Fig. 3 for scatter plots of WMH and cognitive function in relation to hippocampus volumes).

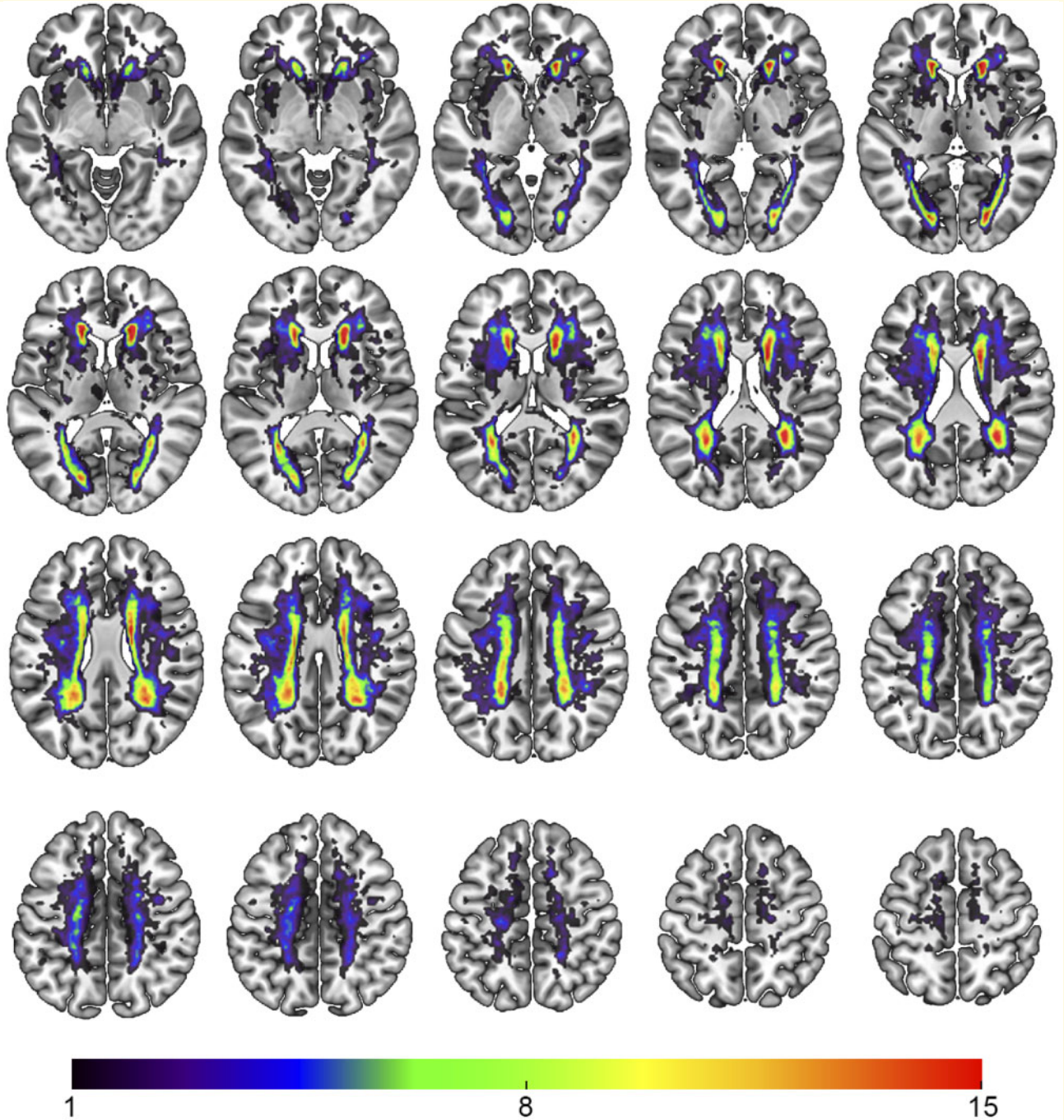

Figure 2 WMH probability map of all participants. Colour indicates the number of participants with lesions in the corresponding voxel. Lesions were mostly found in periventricular white matter. Radiological convention.

Reduction in whole-brain functional connectivity

Whole-brain functional connectivity calculated by the imaginary coherence was assessed in a 90 × 90 ROI connectome based on the automated anatomical labelling atlas. In an exploratory approach, we performed multiple linear regression analyses in order to investigate the impact of WMH lesion load on functional connectivity, corrected for age. We iteratively tested the model for each frequency band (delta, theta, alpha and beta) and each connection (4005 connections). With increasing lesion load, alpha connectivity decreased. The decrease was significant in long-range connections, spanning across lobes, e.g., from frontal regions to temporal, insular, subcortical, central, parietal and occipital lobe (FDR

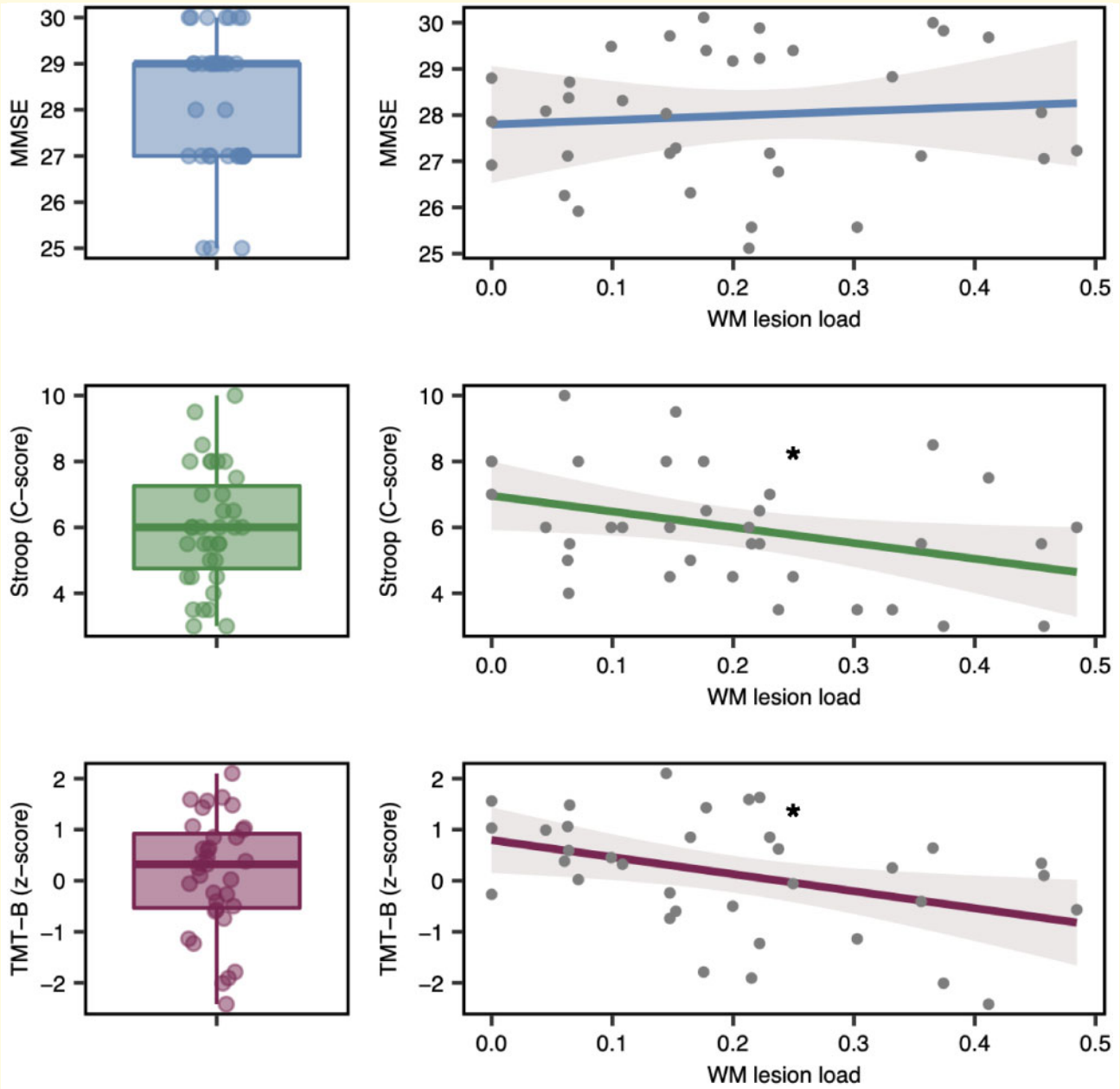

Figure 3 Cognitive scores and its relationship to WMH lesion load. Left column: Results of cognitive testing for MMSE, Stroop (C-score) and TMT-B (z-score). Boxplots depict median and 25%/75% quantile; points show individual data. Right column: Effect plot of linear model analyses to assess cognition as a function of WMH lesion load. Three separate models for MMSE, Stroop and TMT-B tests were calculated. The model MMSE was corrected for age, Stroop C-scores as well as TMT-B z-scores were already transformed based on age, sex and level of education. Line depicts the prediction line, with a 95% confidence band and partial residuals. With increasing lesion load executive functions (Stroop, TMT-B) decline, global cognitive performance (MMSE) does not show an effect based on lesion load. Asterisks mark the level of significance, $*p < 0.05$.

corrected for connections = 4005, $P_{corrected} < 0.1$, Fig. 5A). No single connection within one lobe showed a significant relationship to the lesion load ratio, supporting the notion that the connectivity decrease associated with WMH lesions predominantly affects long-range connections (Fig. 5). In these models, the fixed effect 'age' did not predict alpha connectivity after correction for multiple comparisons. In order to analyse the effect of functional connectivity not for each connection individually but for the whole significant network, we performed an additional linear-mixed model analysis. The linear-mixed model analysis with additional random effects for

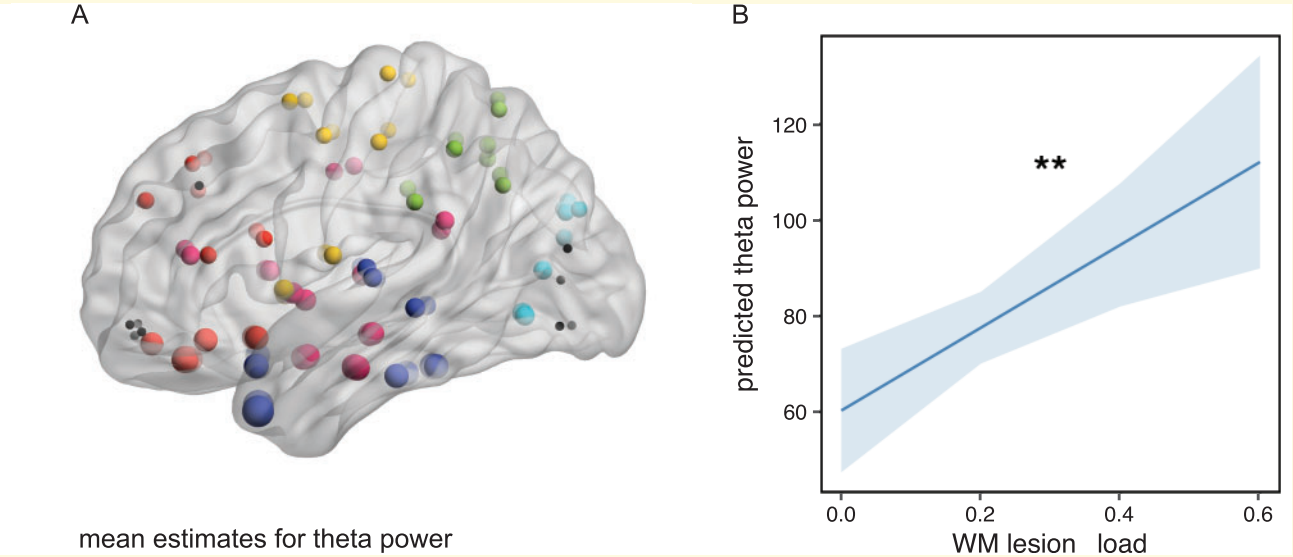

Figure 4 Theta power as a function of WMH lesion load. (**A**) Mean model estimates for theta power as a function of WMH lesion load corrected for age. Dots mark the centre of gravity of each ROI. Size of dot represents the mean model estimate for theta power. Coloured dots depict models, in which the *P*-value of the overall model as well as the *P*-value of the effect 'WMH lesion load' is significant (FDR corr. $P < 0.05$). Black dots are ROIs that are not significant. Colour of dots represents the belonging to a region. Blue = temporal lobe, red = frontal lobe, yellow = central area, green = parietal lobe, turquoise = occipital lobe, magenta = insular and subcortical. (*B*) Effect plot of factor 'WMH lesion load 'for linear-mixed model analysis including all ROIs. Line displays the prediction line, shaded area the 95% confidence interval. $^{**}P < 0.01$. With increasing WMH lesion load the theta power increases globally.

significant connections and by-patient variability, confirmed a decrease of functional connectivity with increasing lesion load [$F(1,35) = 7.86$, $P = 0.0082$, Fig. 5C]. Neither delta, theta nor beta band connectivity showed a significant relationship to WMH lesion load. When calculating the linear-mixed model further including cognitive function as a fixed effect (either MMSE, TMT-B or Stroop) the fixed effect 'cognitive function' was not significant, hence the decrease of functional connectivity did not depend on cognitive function.

Discussion

In our study, we analysed the impact of white matter lesion load in cerebral SVD on oscillatory power and functional brain connectivity measured with high-density resting-state EEG. We leveraged source reconstruction methods and found an increase of theta power in relationship to white matter lesion load, independently of age. Moreover, whole-brain functional connectivity revealed a disrupted network most pronounced in long-range connections connected to the frontal lobe, associated with WMH in patients without clinical signs of mild cognitive impairment or dementia.

In clinical EEG, the presence of temporal theta waves is well known to increase in the older population (Schomer and Silva, 2010); however, when controlling for risk factors of brain dysfunction, age-associated EEG changes are very subtle even in the very old (Shigeta *et al.*, 1995). In our cohort, participants with a greater white matter lesion load showed an increase of theta power. Importantly, this increase in power was independent of age. The increase was evident in virtually all brain regions, sparing only superior orbitofrontal regions as well as the rostral part of the occipital cortex. Theta power was highest in the limbic system and the temporal lobe. Theta oscillations are a key mechanism for the information processing in hippocampus and invasive-EcoG studies in patients have linked the well-studied hippocampal theta in rodents to human behaviour (Kahana *et al.*, 2001). The power of theta oscillations has been shown to increase during cognitive tasks and might reflect attention and cortical control (Kahana, 2006). These slow rhythms synchronize widespread neuronal ensembles by transient coupling with higher frequency localized oscillations (Buzsáki and Draguhn, 2004). It has been shown, that higher theta amplitude results in a stronger high gamma–theta coupling (Canolty *et al.*, 2006). Hence, one might speculate that the increase in theta amplitude in patients with WMH from cerebral SVD represents a compensatory mechanism in order to enhance coordinated activity in distributed cortical areas as a mechanism for communication during cognitive processing. On the contrary, previous EEG studies looking at oscillatory power in patients with subcortical vascular dementia found an increase of low-frequency power, accompanied by a reduction of alpha and beta power (Gawel *et al.*, 2007; van Straaten *et al.*, 2012), associated with a worsening of cognition function. These data might suggest that the

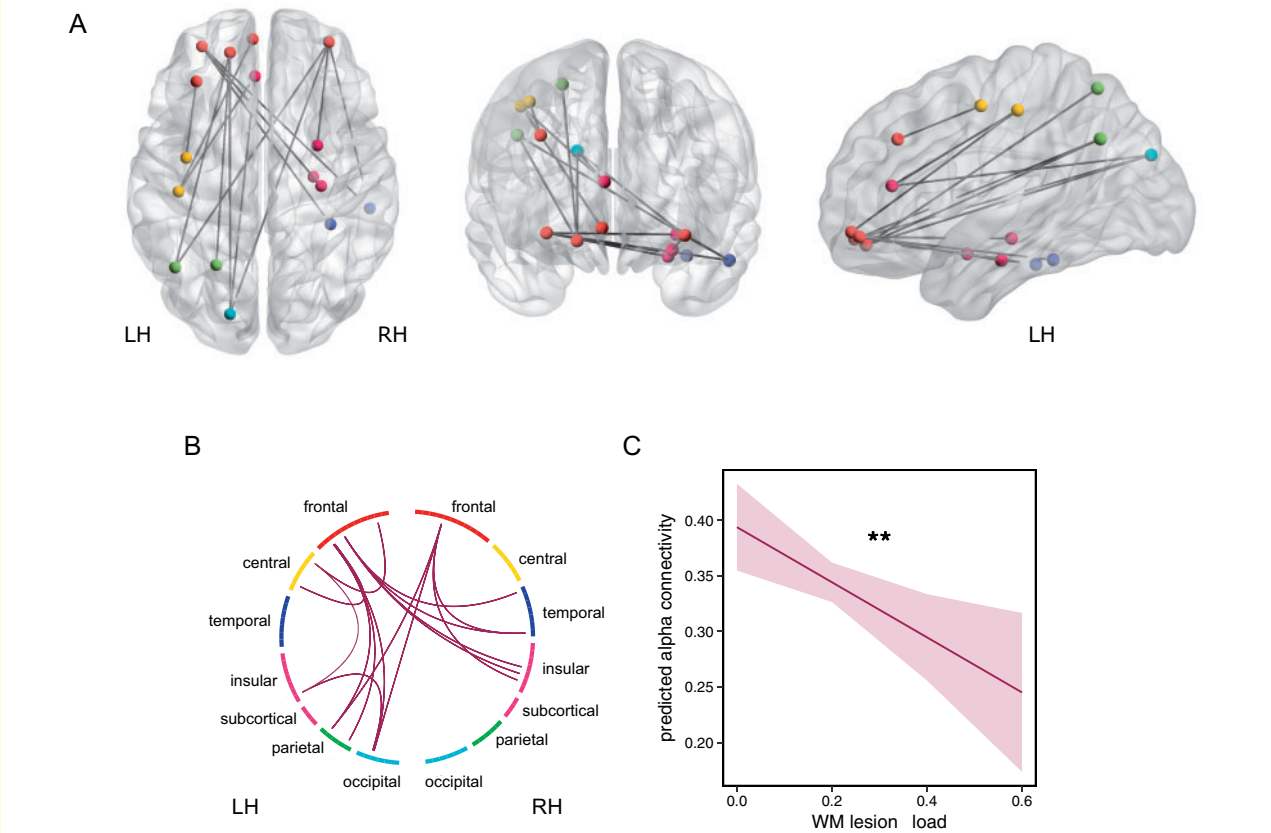

Figure 5 Functional connectivity as a function of WMH lesion load. (**A**) Significant edges of alpha connectivity as a function of WMH lesion load corrected for age. Dots mark the centre of gravity of each ROI that has a significant connection. (**B**) Circular plot of significant alpha connections. Each coloured section represents one lobe/region. Circular plot confirms that no connection within one lobe is significant. Colour of dots in (**A**) and section in (A) represent the belonging to a lobe/region. Blue = temporal lobe, red = frontal lobe, yellow = central area, green = parietal lobe, turquoise = occipital lobe, magenta = insular and subcortical. LH = left hemisphere, RH = right hemisphere. (**C**) Effect plot of factor 'WMH lesion load 'for linear-mixed model analysis including all significant alpha connections. Line displays the prediction line, shaded area the 95% confidence interval. $^{**}P < 0.01$. With increasing WMH lesion load the alpha connectivity decreases.

increase in low-frequency power could already mark a breakdown of the system rather than a compensation. It remains unclear, however whether the decline in cognitive performance is due to the increase of low-frequency power or due to the reduction of alpha and beta power.

Slowing of the EEG with an increase in delta/theta power as well as a decrease of alpha/beta power has been extensively reported in other neurodegenerative diseases, especially in Alzheimer's Disease (Riekkinen *et al.*, 1991; Jeong, 2004). In Alzheimer's Disease, dysregulation of cholinergic basal forebrain neurons that project primarily to central limbic structures, but also to widespread cortical areas, might play a critical role in the pathological oscillatory theta changes (Steriade *et al.*, 1990; Jeong, 2004). The involvement of cholinergic dysfunction has also been debated in vascular dementia (Mesulam *et al.*, 2003; Engelhardt *et al.*, 2007). Here, rather than a dysregulation of cholinergic basal forebrain neurons, subcortical lesions might interrupt ascending cholinergic axons crossing within the hemispheric white matter. Our finding, that theta power depends on WMH lesion load but not hippocampal volume, further supports this notion.

We assessed whole-brain functional connectivity in relationship to white matter disease. A higher white matter lesion load was associated with a decrease of alpha-band connectivity. The decrease of functional connectivity was evident in long-range connections, mostly originating or terminating in the frontal lobe. In line with this observation, WMH most frequently affect the periventricular and subcortical regions which comprise long white matter tracts connecting distant brain regions. Moreover, no short-range connection within one lobe showed a significant decrease in connectivity in relationship to

leukoaraiosis. Accordingly, subcortical u-fibres as well as local association fibers are initially spared in small vessel ischaemic white matter lesions (Pantoni and Garcia, 1997).

An impairment of the frontoparietal network in cerebral SVD was also reported in resting-state fMRI studies (Schaefer *et al.*, 2014). Moreover, higher tract specific white matter lesion load has been shown to be related to lower functional connectivity in the corresponding brain regions (Langen *et al.*, 2017). Apart from functional changes, previous studies have observed a decline of structural connectivity in SVD patients (Lawrence *et al.*, 2014; Kim *et al.*, 2015; Tuladhar *et al.*, 2016). A very similar pattern of disrupted connectivity as shown in our study has been observed with diffusion tensor imaging in a cohort of patients with symptomatic SVD (Lawrence *et al.*, 2014). In accordance to the impaired network of alpha connectivity, the structural subnetwork impaired in patients with SVD comprised predominantly prefrontal cortex, parietal and temporal regions as well as frontal and precuneus pathways to basal ganglia, limbic and insular regions. The disproportionate involvement of prefrontal connectivity, that was also evident in our study, provides a potential explanation for the deficits of executive function that are characteristic for vascular cognitive impairment (Román *et al.*, 2002). Multiple studies have related cognitive functions to white matter lesion load as well as structural (Tuladhar *et al.*, 2016; Langen *et al.*, 2018) and functional (Papma *et al.*, 2013) network disruptions. In our study, we found worse executive function with increasing lesion load. Cognitive function, including executive function, was not associated with spectral power or functional connectivity. We speculate that mild cognitive dysfunction was too subtle to show a correlation with functional connectivity levels measured from neural oscillatory activity.

Connectivity changes in relationship to white matter lesion load were restricted to the alpha band. Faster oscillatory components, such as beta oscillations reflect more local processing with cortico-cortical connections (Pfurtscheller and Lopes da Silva, 1999), hence might not be as affected by white matter disease. On the contrary, alpha oscillations are generated through the interaction of thalamocortical and cortico-cortical systems with strong modulation from many subcortical regions (Steriade *et al.*, 1990; Crunelli *et al.*, 2018), which render them more susceptible to subcortical white matter pathology. Alpha oscillatory networks have been shown to play an important role in information processing and impact cognitive performance. Multimodal studies have linked alpha activity to the intrinsic cognitive control networks (Sadaghiani and Kleinschmidt, 2016). Hence, we speculate, that alterations of alpha-band connectivity in patients with WMH might serve as a precursor of network-failure that with increasing severity, might cause cognitive decline. In Alzheimer's Disease, apart from a decrease of coherence in the alpha band, beta band connectivity is also locally diminished (Jeong, 2004), again underlying the difference of Alzheimer's Disease as a neocortical disconnection syndrome and cSVD, a disease mostly characterized by subcortical white matter pathology.

There are limitations to our study. Even though we selected participants that did not self-report any cognitive impairment, after study inclusion, three participants presented with an MMSE of 25, already pointing to mild dementia. In addition, MMSE is prone to false-negative results in patients with mild cognitive impairment, limiting the general conclusion that patients did not present with cognitive impairments. Furthermore, we cannot exclude the co-occurrence of other neurodegenerative pathologies, as they are a frequent finding in patients with cerebrovascular pathology (Gorelick *et al.*, 2011). We did show, however, that hippocampus volume did not influence theta power, supporting the notion that oscillatory changes were due to WMH but not hippocampal atrophy. Another point concerns the correction for multiple comparisons in a high-dimensional space of cortio-cortical interactions. Correction can conceal weaker but functionally relevant connections, hence we did only correct for ROIs but not frequency bands, and in case of 4005 connections set the FDR rate to 0.1. Moreover, the size of study cohort, especially participants with no global cognitive impairment and extensive lesion load is small, limiting the generalizability of our results and carrying the risk of a selection bias.

In conclusion, patients with greater white matter lesion load showed an increase in global theta power that was independent of age. Whole-brain functional connectivity revealed a disrupted alpha band network most pronounced in long-range connections connected to the frontal lobe preceding pronounced cognitive impairment. Hence, oscillatory neuronal network changes due to white matter lesions might be sensible to subtle cognitive impairments that are not yet clinically relevant.

Supplementary material

Supplementary material is available at *Brain Communications* online.

Funding

This work was supported by a grant from the German Research Foundation (Deutsche Forschungsgemeinschaft, DFG) Sonderforschungsbereich (SFB) 936, Project C1 (C.G.) and C2 (G.T.).

Competing interests

The authors report no competing interests.

References

Buzsáki G, Draguhn A. Neuronal oscillations in cortical networks. Science 2004; 304: 1926–9.

Canolty RT, Edwards E, Dalal SS, Soltani M, Nagarajan SS, Kirsch HE, et al. High gamma power is phase-locked to theta oscillations in human neocortex. Science 2006; 313: 1626–8.

Carmichael O, Schwarz C, Drucker D, Fletcher E, Harvey D, Beckett L, et al. Longitudinal changes in white matter disease and cognition in the first year of the Alzheimer disease neuroimaging initiative. Arch Neurol 2010; 67: 1370–8.

Clas P, Groeschel S, Wilke M. A semi-automatic algorithm for determining the demyelination load in metachromatic leukodystrophy. Acad Radiol 2012; 19: 26–34.

Crunelli V, Lőrincz ML, Connelly WM, David F, Hughes SW, Lambert RC, et al. Dual function of thalamic low-vigilance state oscillations: rhythm-regulation and plasticity. Nat Rev Neurosci 2018; 19: 107–18.

Engelhardt E, Moreira DM, Laks J. Vascular dementia and the cholinergic pathways. Dement Neuropsychol 2007; 1: 2–9.

Fischl B, Salat DH, Busa E, Albert M, Dieterich M, Haselgrove C, et al. Whole brain segmentation: automated labeling of neuroanatomical structures in the human brain. Neuron 2002; 33: 341–55.

Fuchs M, Kastner J, Wagner M, Hawes S, Ebersole JS. A standardized boundary element method volume conductor model. Clin Neurophysiol 2002; 113: 702–12.

Gawel M, Zalewska E, Szmidt-Sałkowska E, Kowalski J. Does EEG (visual and quantitative) reflect mental impairment in subcortical vascular dementia? J Neurol Sci 2007; 257: 11–6.

Gorelick PB, Scuteri A, Black SE, DeCarli C, Greenberg SM, Iadecola C, et al. Vascular contributions to cognitive impairment and dementia: a statement for healthcare professionals from the American Heart Association/American Stroke Association. Stroke 2011; 42: 2672–713.

Gu Z, Gu L, Eils R, Schlesner M, Brors B. circlize Implements and enhances circular visualization in R. Bioinforma Oxf Engl 2014; 30: 2811–2.

Habes M, Erus G, Toledo JB, Zhang T, Bryan N, Launer LJ, et al. White matter hyperintensities and imaging patterns of brain ageing in the general population. Brain J Neurol 2016; 139: 1164–79.

Jenkinson M, Beckmann CF, Behrens TEJ, Woolrich MW, Smith SM. FSL. NeuroImage 2012; 62: 782–90.

Jeong J. EEG dynamics in patients with Alzheimer's disease. Clin Neurophysiol 2004; 115: 1490–505.

Kahana MJ. The cognitive correlates of human brain oscillations. J Neurosci 2006; 26: 1669–72.

Kahana MJ, Seelig D, Madsen JR. Theta returns. Curr Opin Neurobiol 2001; 11: 739–44.

Kim HJ, Im K, Kwon H, Lee J-M, Kim C, Kim YJ, et al. Clinical effect of white matter network disruption related to amyloid and small vessel disease. Neurology 2015; 85: 63–70.

Langen CD, Cremers LGM, de Groot M, White T, Ikram MA, Niessen WJ, et al. Disconnection due to white matter hyperintensities is associated with lower cognitive scores. NeuroImage 2018; 183: 745–56.

Langen CD, Zonneveld HI, White T, Huizinga W, Cremers LGM, de Groot M, et al. White matter lesions relate to tract-specific reductions in functional connectivity. Neurobiol Aging 2017; 51: 97–103.

Lawrence AJ, Chung AW, Morris RG, Markus HS, Barrick TR. Structural network efficiency is associated with cognitive impairment in small-vessel disease. Neurology 2014; 83: 304–11.

de Leeuw F-E. Prevalence of cerebral white matter lesions in elderly people: a population based magnetic resonance imaging study. The Rotterdam Scan Study. J Neurol Neurosurg Psychiatry 2001; 70: 9–14.

Makeig S, Bell AJ, Jung T-P, Sejnowski TJ. Independent component analysis of electroencephalographic data [Internet]. Adv Neural Inf Process Syst 8 MIT Press Camb MA 1996; 145–51.

Mesulam M, Siddique T, Cohen B. Cholinergic denervation in a pure multi-infarct state: observations on CADASIL. Neurology 2003; 60: 1183–5.

Nolte G, Bai O, Wheaton L, Mari Z, Vorbach S, Hallett M. Identifying true brain interaction from EEG data using the imaginary part of coherency. Clin Neurophysiol 2004; 115: 2292–307.

Oken BS, Kaye JA. Electrophysiologic function in the healthy, extremely old. Neurology 1992; 42: 519–26.

Oostenveld R, Fries P, Maris E, Schoffelen J-M. FieldTrip: open source software for advanced analysis of MEG, EEG, and invasive electrophysiological data. Comput Intell Neurosci 2011; 2011: 1–9.

Oswald W, Fleischmann U. Das Nürnberger-Alters-Inventar. 4th ed. Göttingen: Hogrefe; 1997.

Pantoni L. Cerebral small vessel disease: from pathogenesis and clinical characteristics to therapeutic challenges. Lancet Neurol 2010; 9: 689–701.

Pantoni L, Garcia JH. Pathogenesis of leukoaraiosis: a review. Stroke 1997; 28: 652–9.

Papma JM, den Heijer T, de Koning I, Mattace-Raso FU, van der Lugt A, van der Lijn F, et al. The influence of cerebral small vessel disease on default mode network deactivation in mild cognitive impairment. NeuroImage Clin 2013; 2: 33–42.

Pfurtscheller G, Lopes da Silva F. Event-related EEG/MEG synchronization and desynchronization: basic principles. Clin Neurophysiol 1999; 110: 1842–57.

Quandt F, Bönstrup M, Schulz R, Timmermann J, Zimerman M, Nolte G, et al. Spectral variability in the aged brain during fine motor control. Front Aging Neurosci 2016; 8: 305.

Quandt F, Fischer F, Schröder J, Heinze M, Kessner SS, Malherbe C, et al. Normalization of reduced functional connectivity after revascularization of asymptomatic carotid stenosis. J Cereb Blood Flow Metab 2019; 271678X19874338. doi: 10.1177/0271678X19874338.

Riekkinen P, Buzsaki G, Riekkinen P, Soininen H, Partanen J. The cholinergic system and EEG slow waves. Electroencephalogr Clin Neurophysiol 1991; 78: 89–96.

Román GC, Erkinjuntti T, Wallin A, Pantoni L, Chui HC. Subcortical ischaemic vascular dementia. Lancet Neurol 2002; 1: 426–36.

Sadaghiani S, Kleinschmidt A. Brain networks and α-oscillations: structural and functional foundations of cognitive control. Trends Cogn Sci 2016; 20: 805–17.

Schaefer A, Quinque EM, Kipping JA, Arélin K, Roggenhofer E, Frisch S, et al. Early small vessel disease affects frontoparietal and cerebellar hubs in close correlation with clinical symptoms—a resting-state fMRI study. J Cereb Blood Flow Metab 2014; 34: 1091–5.

Schomer DL, Silva FD. Niedermeyer's electroencephalography: basic principles, clinical applications, and related fields. 6th Revised edn. Philadelphia: Lippincott Williams & Wilki; 2010.

Shigeta M, Julin P, Almkvist O, Basun H, Rudberg U, Wahlund LO. EEG in successful aging; a 5 year follow-up study from the eighth to ninth decade of life. Electroencephalogr Clin Neurophysiol 1995; 95: 77–83.

Steriade M, Gloor P, Llinás RR, Lopes da Silva FH, Mesulam M-M. Basic mechanisms of cerebral rhythmic activities. Electroencephalogr Clin Neurophysiol 1990; 76: 481–508.

van Straaten ECW, den Haan J, de Waal H, van der Flier WM, Barkhof F, Prins ND, et al. Disturbed phase relations in white matter hyperintensity based vascular dementia: an EEG directed connectivity study. Clin Neurophysiol 2015; 126: 497–504.

van Straaten ECW, de Haan W, de Waal H, Scheltens P, van der Flier WM, Barkhof F, et al. Disturbed oscillatory brain dynamics in subcortical ischemic vascular dementia. BMC Neurosci 2012; 13: 85.

Tuladhar AM, van Dijk E, Zwiers MP, van Norden AGW, de Laat KF, Shumskaya E, et al. Structural network connectivity and cognition in cerebral small vessel disease. Hum Brain Mapp 2016; 37: 300–10.

Tzourio-Mazoyer N, Landeau B, Papathanassiou D, Crivello F, Etard O, Delcroix N, et al. Automated anatomical labeling of activations

in SPM using a macroscopic anatomical parcellation of the MNI MRI single-subject brain. NeuroImage 2002; 15: 273–89.

Van Veen BD, van Drongelen W, Yuchtman M, Suzuki A. Localization of brain electrical activity via linearly constrained minimum variance spatial filtering. IEEE Trans Biomed Eng 1997; 44: 867–80.

Wardlaw JM, Smith EE, Biessels GJ, Cordonnier C, Fazekas F, Frayne R, et al. Neuroimaging standards for research into small vessel disease and its contribution to ageing and neurodegeneration. Lancet Neurol 2013; 12: 822–38.

Xia M, Wang J, He Y. BrainNet viewer: a network visualization tool for human brain connectomics. PLoS One 2013; 8: e68910.